polymer

Crystallization kinetics and solidified structure in iPP under high cooling rates

I. Coccorullo, R. Pantani*, G. Titomanlio

Department of Chemical and Food Engineering, University of Salerno, Via Ponte don Melillo, 84084 Fisciano SA, Italy

Abstract

A wide set of isothermal and non-isothermal crystallization experiments were carried out in this work on an iPP resin. Several experimental techniques were adopted in order to characterize crystallization kinetics and final morphology of the material, also under cooling rates comparable to those encountered during material processing (up to several hundred K/s). The whole set of data was taken as a reference to identify a kinetic model which describes the evolution of the structural organization of iPP (α crystalline phase and mesomorphic phase) as a parallel of two non-interacting kinetic processes competing for the available amorphous volume. Kolmogoroff equation was adopted to describe the crystallization of the α form. Avrami–Evans–Nakamura isokinetic approach was adopted to describe the evolution of the mesomorphic phase. Resulting kinetic model satisfactorily describes the whole set of experimental data including those obtained on samples solidified under high cooling rates, and reveals that a correct description of the evolution of the α phase during solidification can be attained only if the evolution of the competing mesomorphic phase is kept into account. The effect of cooling rate during solidification from the melt on diameters of spherulites, observed on solidified samples, is also satisfactorily described by model predictions.
© 2002 Elsevier Science Ltd. All rights reserved.

Keywords: Crystallization kinetics; Isotactic polypropylene; Nucleation

1. Introduction

The most widespread processes for the production of polymeric objects include a step in which the molten polymer cools down to a solid. During solidification, semi-crystalline polymers undergo a melt-to-crystal transition with formation of a structure that, in quiescent melts, is often typified by spherulites. Morphological characteristics, which are essentially dictated by the degree of crystallinity and dimensions of spherulites, are affected by the conditions under which solidification takes place. Of course, all characteristics of final product (mechanical, but also transport and optical properties and dimensional stability) are dictated by the molecular organization attained in the solid state. This implies that optimization of processes toward products of superior quality needs a deep understanding and a suitable modeling of the crystallization process, focused on the achievement of quantitative prediction of morphological characteristics.

A number of mathematical models have been proposed for the simulation of quiescent crystallization [1–4]. Most of non-isothermal crystallization theories have been developed on the basis of the Avrami theory for isothermal crystallization. Nakamura et al. [3] extended the theories of isothermal crystallization of Avrami and Evans to non-isothermal case by adopting an isokinetic hypothesis. As often mentioned in the literature, the isokinetic approach does not describe details of structure formation. The well-known experience that, with many polymers, the number of spherulites in the final solid sample increases strongly with increasing cooling rate, is indeed not taken into account by this approach [5].

Kolmogoroff model [5] for the description of crystallization kinetics, identifies an approach which allows to describe also morphological characteristics of the solidified sample. According to this model, crystallinity evolution is described accounting of number of nuclei per unit volume and spherulitic growth rate. Parameters of Kolmogoroff model are usually determined by standard experimental techniques as calorimetric tests and optical microscopy. However, standard tests are always limited to isothermal

* Corresponding author. Tel.: +39-089-964013; fax: +39-089-964057.
E-mail address: rpantani@unisa.it (R. Pantani).

Nomenclature

t_{05}	half time of kinetic process (s)
T_{peak}	peak temperatures during DSC ramps (K)
λ	latent heat of crystallization (J/g)
T_m	melting temperature (K)
χ_α	volume fraction (crystallinity degree) of α phase
χ_{meso}	volume fraction of mesomorphic phase
$\chi_{m,\alpha}$	maximum value of volume fraction (crystallinity degree) of α phase
$\chi_{m,meso}$	maximum value of volume fraction of mesomorphic phase
ρ	density of sample (g/cm^3)
ρ_α	density of α phase (g/cm^3)
ρ_{meso}	density of mesomorphic phase (g/cm^3)
$\rho_{amorphous}$	density of amorphous phase (g/cm^3)
ξ_α	normalized volume fraction (relative crystallinity degree) of α phase $\chi_\alpha/\chi_{m,\alpha}$
ξ_{meso}	normalized volume fraction of mesomorphic phase $\chi_m/\chi_{m,meso}$
N	nucleation density (nuclei/m^3)
G	spherulites growth rate (μm/s)
$N_{a,final}$	final number of active nuclei
R	spherulites radius (μm)

conditions or to cooling rates (a few K/min) that are unacceptably low with respect to those experienced by the material in actual processing conditions (tens or often hundreds of K/s).

Besides the well known observation that, in quiescent condition, the amorphous phase and usually two crystalline phases, α and mesomorphic, are observed in iPP (α crystalline form prevails at low cooling rates and mesomorphic form prevails at high cooling rates [6]), it is also known that, on increasing cooling rate, crystallinity degree decreases and the number of nuclei increases.

In order to obtain a reliable kinetic model to describe crystallinity evolution under processing conditions all these phenomena must be taken into account and, indeed, many efforts have been recently spent along this direction [7–16]. In particular the effect of high cooling rates was analyzed in a series of works conducted at University of Palermo [7–10] and Salerno [11,12], in which the morphology of samples solidified under high cooling rates (several hundreds of K/s) was studied. Magill, Ding and Spruiell [14] measured on-line crystallinity evolution during cooling at moderate cooling rates (up to about 3 K/s) by means of optical methods. This approach was recently extended by Tito-manlio and co-workers to higher cooling rates (30 K/s) [16].

In this work a very wide set of isothermal and non-isothermal crystallization experiments are carried out in order to characterize crystallization kinetics and final morphology of an iPP resin, also under cooling rates comparable to those encountered during material proces-

sing. The whole set of data is analyzed to identify a kinetic model which, keeping into account the presence of several phases, is able to give information about morphological characteristics of the polymer after solidification in a wide range of cooling rates.

2. Experimental

2.1. Material

A commercial grade iPP resin (T30G, $M_w = 481,000$, $M_n = 75,000$, tacticity = 87.6%mmmm), kindly supplied by Montell (Ferrara, Italy), was adopted for the experiments in this work.

2.2. Calorimetry

Standard calorimetric characterization (adopting both isothermal and non-isothermal tests) was performed by means of a DSC apparatus (Mettler) with liquid nitrogen as cooling fluid. Calorimetric data were corrected, to keep into account the low heat transfer coefficient of the polymer, according to the procedure illustrated by Eder et al. [5]. At the beginning of each test the samples were kept for about 30 min at 503 K, with the aim of erasing the effect of previous thermal histories.

Seven samples were analyzed under isothermal conditions. The material was tested at the following temperatures: 394, 396, 398, 400, 403, 405 and 407 K. At higher temperatures, testing times were very high and output signals too low, whereas lower temperatures could not be reached because of the limited apparatus cooling rate, which was not sufficient to prevent samples from crystallizing during cooling to test temperature. The overall energy released during each isothermal test was always found as about 105 J/g. Half time of crystallization ($t_{0.5}$, i.e. the time at which crystallinity reaches one-half of the maximum value) vs temperature for each isothermal test is reported in Fig. 1 (symbols represent experimental data). As expected, in the range of temperatures analyzed in this work, the half time of crystallization increases with the temperature of the isothermal test.

Some samples were subjected to calorimetric tests under cooling rates ranging in the interval 1–60 K/min. Temperatures of the peaks detected by the calorimeter during the tests (T_{peak}) are reported in Fig. 2 vs cooling rate (symbols represent experimental data). It decreases about linearly on a semi-log scale, on increasing cooling rate. Overall heat released during the same tests did not change significantly by changing cooling rate, being always about 105 J/g, consistently with the values found from isothermal tests. This confirms that, even at the maximum cooling rate attainable by the DSC apparatus, the material always reaches the maximum degree of crystallinity.

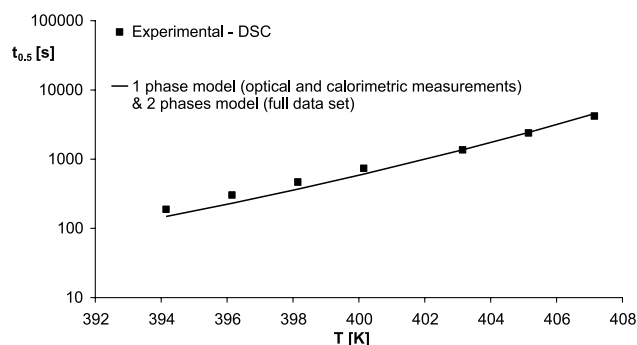Final crystallinity degree of the samples solidified during

Fig. 1. Comparison between experimental determinations of half time of crystallization during DSC isothermal tests (symbols) and predictions performed by the model (lines), adopting parameters listed in Tables 1 (1 phase model) and 2 (2 phases model).

DSC ramps, calculated from calorimetric curves by using $\lambda = 8.7$ J/mol as latent heat of crystallization [15], was always found to be between 48 and 53%. DSC measurements were also adopted to determine material melting temperature, according to the method developed by Marand and co-workers [17], as $T_m = 467$ K.

2.3. Quenching of thin samples and their characterization

Standard characterization methods for crystallization kinetics are limited to isothermal conditions and low cooling rates. In order to investigate the effect of high cooling rates on crystallization, thin films were subjected to fast cooling while a careful measurement of sample thermal history was performed. Final solid films were then analyzed.

The experimental apparatus adopted for the cooling procedure was already presented elsewhere [11] and is schematically depicted in Fig. 3. It consists of a sample holder made of two thin copper slabs linked to a rod which can slide vertically bringing the sample from an oven, in the upper part of the apparatus, to the lower part, where a cooling fluid is sprayed against the copper slabs. The two copper slabs were 0.5 mm thick and the thickness of the polymer sample located between them
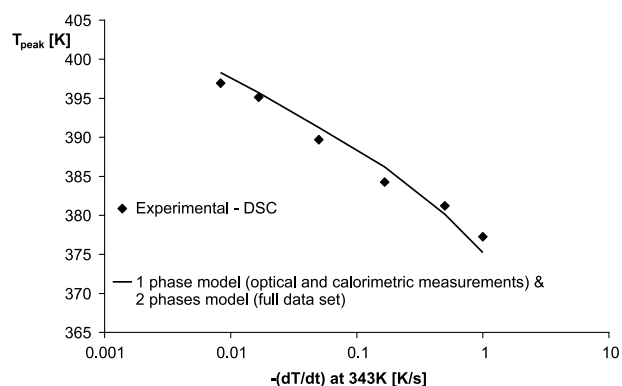

Fig. 2. Comparison between experimental determinations of peak temperatures during DSC cooling ramps (symbols) and predictions performed by the model (lines), adopting parameters listed in Tables 1 (1 phase model) and 2 (2 phases model).
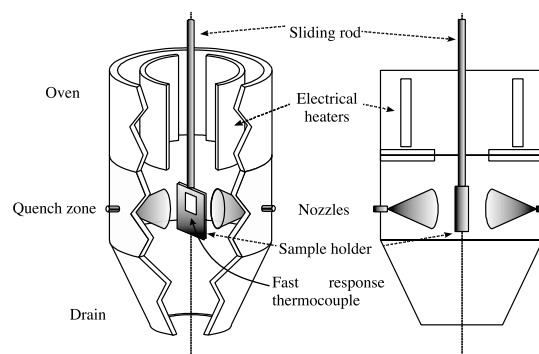

Fig. 3. Layout of the experimental apparatus used for controlled cooling histories.

was always smaller then 0.1 mm; contact between copper walls and polymer was ensured during the whole test by means of elastic pincers. Temperature evolution was monitored by a thin thermocouple located inside the copper holders close to the polymer sample. Values of Biot number were estimated smaller than 0.1 (up to the highest cooling rate attained) with reference to both the polymer sample and the copper sample holder. These values of Biot number assure that internal resistance to heat transfer is negligible with respect to the external one, and thus thermocouple readings can be considered representative of a homogeneous temperature inside the polymer.

Similarly to the samples subjected to calorimetric tests, samples were kept in the 'oven' at 503 K for 30 min and then cooled in the 'quench zone' to room temperature. During the solidification process, measured cooling rates are obviously not constant with temperature, being the driving force essentially dictated by the difference between sample and cooling media temperatures. Cooling histories and cooling rates vs temperature of the tests performed in this work are reported in Fig. 4a and b, respectively. Cooling rate measured at 343 K is chosen as a reference to identify a particular cooling history, as suggested by Titomanlio and coworkers [7] for iPP. Cooling rates calculated according to this criterion ranged between 0.02 and 300 K/s, depending on cooling media adopted (air or water), their values are also reported in Fig. 4b for each test.

2.4. Density measurements

Density of samples solidified in different conditions were measured in density-gradient columns prepared with solutions of ethyl alcohol and water. Density of the samples, about 1 h after cooling procedures, was measured at 298 K.

Data are reported in Fig. 5 (full symbols) and show that density is essentially constant for cooling rates lower than about 20 K/s. For higher cooling rates an abrupt drop of density takes place, consistently with a decrease of final crystallinity degree at these cooling rates.
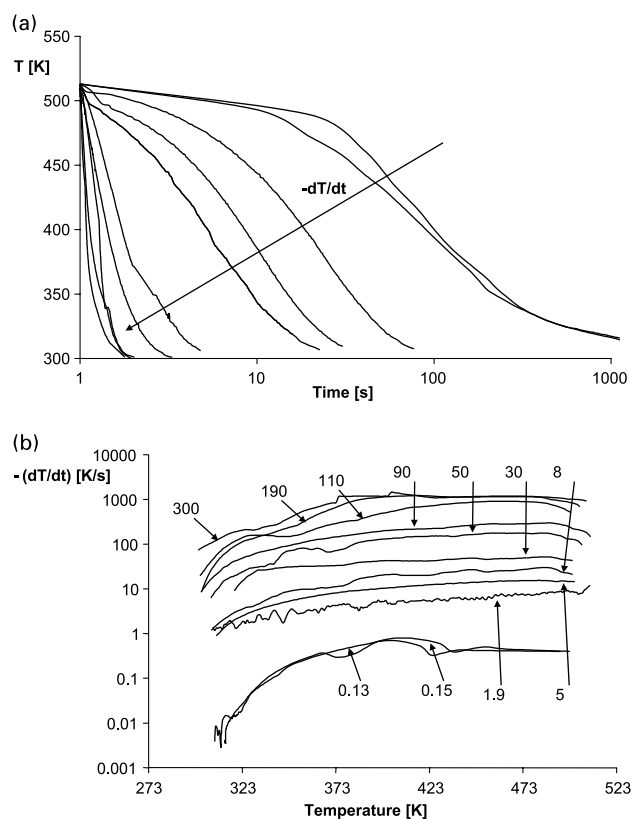
Fig. 4. (a) Cooling histories of samples solidified under controlled cooling rate. (b) Cooling histories of samples solidified under controlled cooling rate. Reported cooling rates were measured at 343 K.

2.5. Wide angle X-ray scattering

Isotactic polypropylene may exist in three different crystalline structures (α monoclinic phase, β hexagonal phase, γ orthorhombic phase), a mesomorphic and an amorphous phase [6]. Every single phase is characterized by several diffractions peaks that appear in well defined positions on a WAXS pattern [6].

α monoclinic phase is often prevalent and it is stable from a thermodynamic point of view. It is the most well-known and studied form of iPP (several literature results are reported by Hieber [18] and Eder [5]). β hexagonal phase is unstable from a thermodynamic point of view and its formation is related to particular conditions of solidification, such as high shear rates and the presence of nucleating agents [19]. γ orthorhombic phase was often found in samples crystallized under very high pressures or in high molecular weight iPP crystallized from isotropic melt [20–22]. When isotactic polypropylene is rapidly quenched from the melt, it forms a phase of intermediate order (between amorphous disorder and crystalline order) usually called mesomorphic phase; its structure and properties have been studied by many authors, but precise nature of this phase is still in debate [6].

In order to determine final content of phases, some quenched samples were analyzed using WAXS.
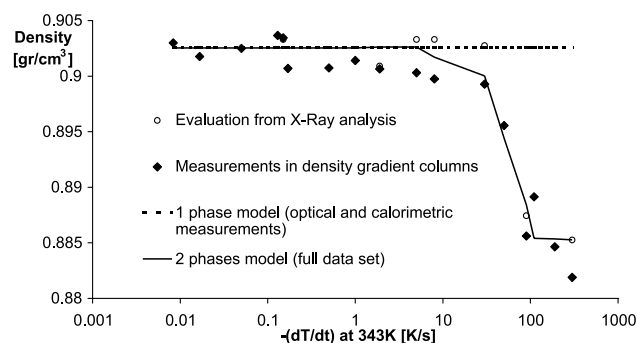

Fig. 5. Comparison between experimental determinations of density of samples solidified under controlled cooling rate (full symbols), evaluated densities on the basis of X-ray measurements (void symbols) and predictions performed by the model (lines), adopting parameters listed in Tables 1 (1 phase model) and 2 (2 phases model).

In spite of the fact that previous studies by a number of investigators [19] have demonstrated that β phase do indeed form in the temperature range investigated in this work, only α, mesomorphic and amorphous phases were detected by analysis of the diffractograms.

WAXS patterns were analyzed by a deconvolution procedure performed according to a scheme reported in Ref. [23] and summarized below. The full spectrum is considered as a superposition of the a number of reflections, due to each phase present (10 reflections were considered: 7 for the α phase, corresponding to $2\theta = 14.1$, 16.9, 18.6, 21.2, 22.1, 25.5 and 28.5; 2 for the mesomorphic form, corresponding to $2\theta = 14.5$ and 21; 1 for the amorphous halo); each reflection being described by a combination of a Lorentzian function and a Gaussian function.

The parameters defining each reflection were determined, with a general purpose optimization routine, adopting as objective function the total quadratic error with respect to the experimental spectrum. Obviously, deconvolution results are affected by some uncertainty, it was estimated as ± 3% on percentage of each phase. Results of deconvolution procedures are shown in Fig. 6a for a sample in which α phase prevails on mesomorphic phase (30 K/s) and in Fig. 6b for a sample which is mainly mesomorphic (300 K/s).

Phase contents vs cooling rate experienced during cooling (as measured at 343 K) are reported in Fig. 7 (symbols represent experimental data): at cooling rates smaller than about 30 K/s, α phase prevails on mesomorphic phase; on increasing cooling rate above 30 K/s, the amount of α phase decreases and that of mesomorphic phase increases, eventually the mesomorphic form prevails on the α phase above about 80 K/s. It is worth noticing that, except for a very narrow range of cooling rates (from 30 to 80 K/s) within which the contents of α and mesomorphic phases are one within 50% of the other, for most cooling conditions one of the phases largely predominates on the other one. The amount of amorphous fraction (not shown in Fig. 7), even if slightly increasing on increasing cooling rate, remains

(a)

Intensity [a.u.]

Experimental
- - - Fitting
—— Alpha phase 2teta=14.1°, 16.9°, 18.6°, 21.2, 22.1, 25.5°, 28.5°
-·-·- Mesomorphic phase 2teta=14.5°,21°
········ Amorphous

2θ

(b)

Intensity [a.u.]

Experimental
- - - Fitting
—— Alpha phase 2teta=14.1∞, 16.9°, 18.6°, 21.2, 22.1, 25.5°, 28.5°
-·-·- Mesomorphic phase 2teta=14.5°,21°
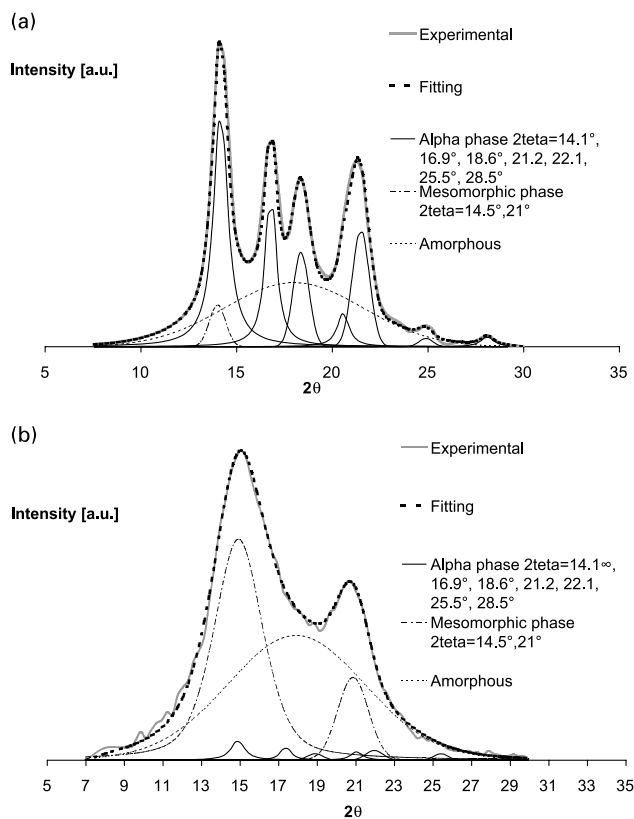········ Amorphous

2θ

Fig. 6. (a) Deconvolution results of sample solidified at 30 K/s. (b) Deconvolution results of sample solidified at 300 K/s.

essentially constant independently on cooling rate [9]. Data also show that maximum percentage for each phase is about 55% for α phase and about 45% for mesomorphic phase. These values will be thus adopted in the following to identify the maximum percentage of each of the two phases, which will be referred to as $\chi_{m,i}$ where 'i' stands either for α or for the mesomorphic phase. It is worth noticing that a value of $\chi_{m,\alpha} = 55\%$ is consistent with DSC results, being α phase the only one present at cooling rates allowed by a DSC apparatus.

The change from α to mesomorphic phase on increasing cooling rate, as found by X-ray analysis, is also consistent with density reduction at high cooling rates as shown in Fig. 5. Indeed sample density at 298 K can be calculated on the basis of α and mesomorphic phases amounts according to a simple mixture rule

$$\rho = \rho_\alpha \chi_\alpha + \rho_{meso} \chi_{meso} + \rho_{amorphous}(1 - \chi_\alpha - \chi_{meso}) \qquad (1)$$

where ρ is the density of the sample, ρ_i and χ_i the density and volume fraction, respectively, of a generic phase 'i', standing either for α or for amorphous or for mesomorphic. (Literature values were given to densities at 298 K of α, mesomorphic and amorphous phases, respectively: $\rho_\alpha = 940$ kg/m^3, $\rho_{meso} = 916$ kg/m^3, $\rho_{am} = 860$ kg/m^3 [6].) Density calculated by Eq. (1) on the basis of volume fractions obtained from deconvolution of WAXD diffractograms nicely compare (open circles in Fig. 5) with

Vol. fraction [ ]

● alpha phase from Xray analysis
▲ mesomorphic phase from Xray analysis
- - - 1 phase model - (optical and calorimetric measurements)
—— alpha - 2 phases model - (full data set)
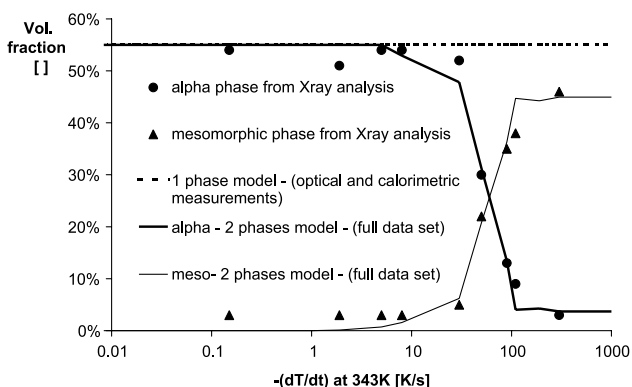—— meso- 2 phases model - (full data set)

-(dT/dt) at 343K [K/s]

Fig. 7. Comparison between experimental determinations (by means of X-ray analysis) of volume fraction of α (circles) and mesomorphic (triangles) phase and predictions performed by the model (lines), adopting parameters listed in Tables 1 (1 phase model) and 2 (2 phases model).

experimental values measured in density gradient columns. Density reduction at high cooling rates is thus to be related to the replacement in the solid sample of the α crystalline phase by the lighter mesomorphic phase.

2.6. Optical and scanning electronic microscopy

In order to determine average diameter of spherulites after a given thermal treatment, samples solidified under different cooling rates were analyzed by polarized light optical microscopy and by scanning electronic microscopy. In order to better detect crystalline morphologies, all samples were chemically etched according to the procedure suggested by Bassett [24]. The etchant used was a solution of potassium permanganate in a mixture of 10:4:1 volumes of concentrated sulphuric acid, orthophosphoric acid and distilled water, respectively (1 g of potassium permanganate in 100 ml of mixture). A 2 h period of etching at room temperature was generally sufficient to reveal the surface topography.

Cross-polarized optical micrographs (left) and scanning electron micrographs (right) of some of the samples obtained using the quenching device depicted in Fig. 3 are reported in Figs. 8 and 9. Micrographs show the effect of cooling rate: spherulites can be clearly detected (both in cross-polarized optical micrographs and in the scanning electron micrographs) in samples obtained at low cooling rates, where α form prevails on mesomorphic phase; on increasing cooling rate, as expected, both the amount of α form and average spherulites diameter decrease. Particularly interesting are the micrographs of the samples solidified at 50 and 90 K/s, in which spherulites appear immersed in a flat matrix; thus in those cases they do not impinge to each other and, as suggested by results of X-rays analysis, are surrounded by a mesomorphic phase.

Diameters of spherulites, as obtained from inspection of scanning electron micrographs, are reported in Fig. 10 for all quenched samples: as expected, the number of spherulites increases and their radius decreases, on
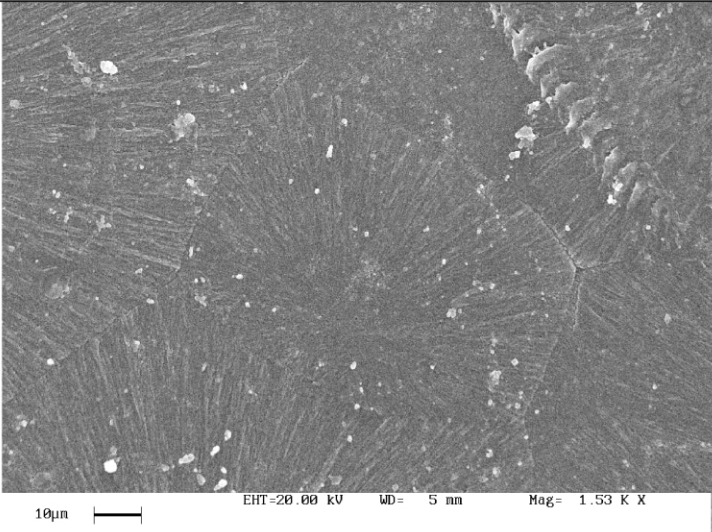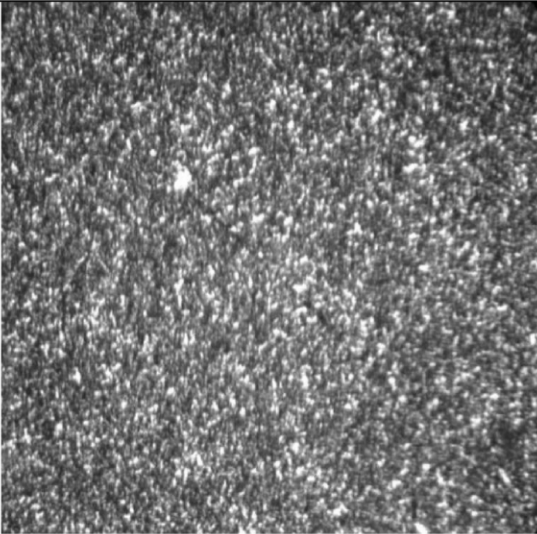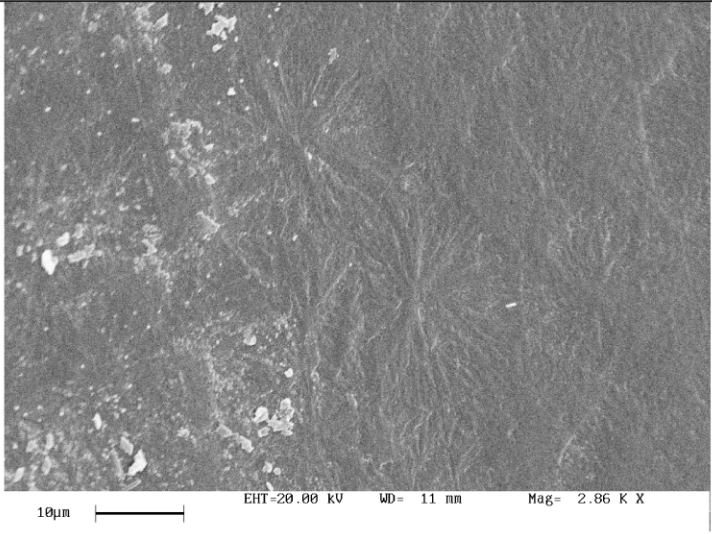
Crossed polarizers optical microscopy	Scanning electronic microscopy
100 μm	10μm EHT=20.00 kV WD= 5 mm Mag= 1.53 K X
POL a	SEM a
Cooling rate at 343K=0.02 K/s	
100 μm	10μm EHT=20.00 kV WD= 11 mm Mag= 2.86 K X
POL b	SEM b
Cooling rate at 343K=2 K/s	

Fig. 8. Micrographs obtained by crossed polarizers optical microscopy and scanning electronic microscopy of some of the samples solidified under controlled cooling rate (0.02 and 2 K/s).
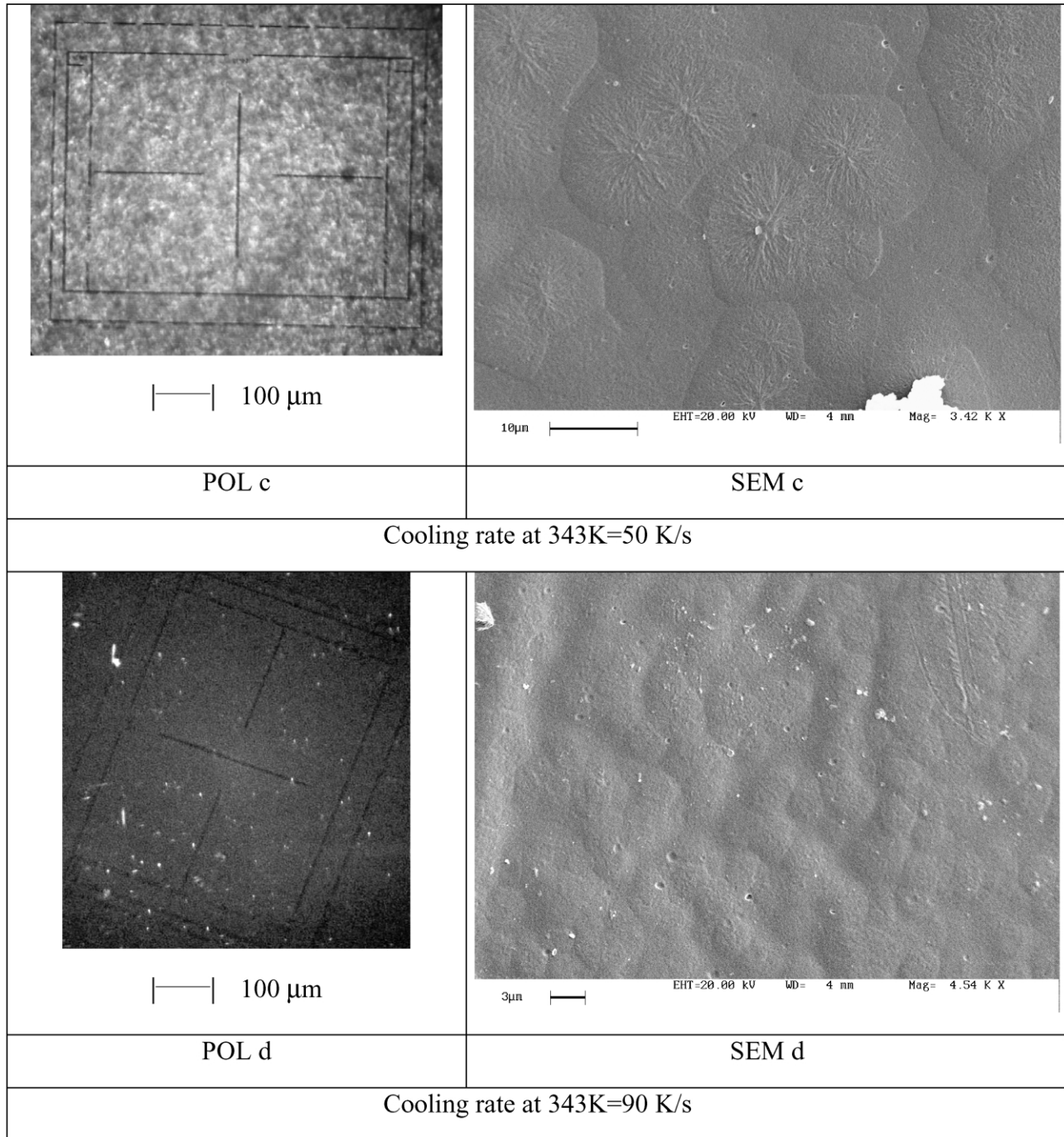
Fig. 9. Micrographs obtained by crossed polarizers optical microscopy and scanning electronic microscopy of some of the samples solidified under controlled cooling rate (50 and 90 K/s).

increasing cooling rate; in particular, diameters decrease from about 90 μm (at a cooling rate of 0.02 K/s) to about 4 μm (at cooling rate of 90 K/s). Spherulites were not detected in samples solidified at cooling rates higher than 100 K/s.

3. Kinetics modeling

As mentioned above, two crystalline phases (α and mesomorphic) and an amorphous phase were detected by WAXS in the solid samples: α phase prevails on the mesomorphic at low cooling rate (smaller than about 20 K/s at 343 K) and mesomorphic phase prevails on α at higher cooling rates. Since the presence of the two crystalline phases influences morphological characteristics and thus final properties of the solid, both of them must obviously be taken into account in the modeling.

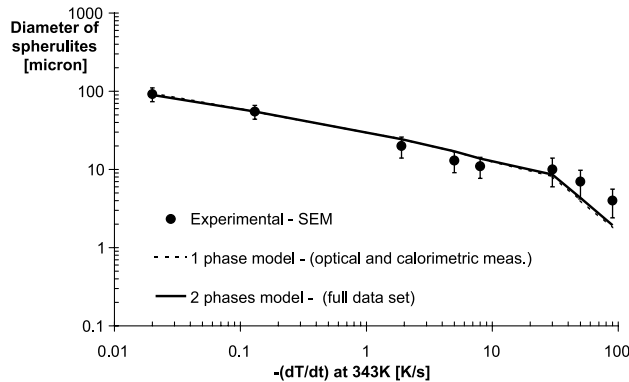In this work a simple kinetic model was adopted

Fig. 10. Comparison between experimental determinations (by SEM analysis) of the diameter of spherulites in samples solidified under controlled cooling rate (symbols) and predictions performed by the model (lines), adopting parameters listed in Tables 1 (1 phase model) and 2 (2 phase model).

assuming a parallel of two non-interacting kinetic processes competing for the available amorphous volume. The model accounts of the fact that each of the crystalline phases, while growing, includes some amorphous portions which limit the maximum reachable crystallinity degree of the considered phase to a value, χ_m, lower than 1. Furthermore, for each crystalline phase, nucleation and growth are allowed only in amorphous regions still free of crystalline structures; thus, if one of the crystalline phases reaches its ultimate crystalline degree, the other one cannot crystallize further (secondary crystallization is not accounted for in the current model formulation). According to Ref. [7] the evolution of the fraction of each of the crystalline phases can thus be described by:

$$\frac{d\xi_i}{dt} = (1 - \xi)\frac{dk_i}{dt} \qquad (2)$$

where the subscript i stands for a particular phase (either for α or *meso* in this work), $\xi_i = \chi_i/\chi_{m,i}$, χ_m being the maximum volume fraction which keeps into account the fact that growing crystals are always embedded into amorphous regions. $\xi = \sum_i \xi_i$ and k_i is the expectancy of volume fraction of each phase if no impingement would occur.

By summing up Eq. (2) over the index 'i', and solving the differential equation, one simply obtains

$$\xi(t) = 1 - \exp[-k(t)] \qquad (3)$$

where $k = \sum_i k_i$. Eq. (3) describes the evolution of the overall crystalline fraction, accounting for all phases formed (α and mesomorphic phases, in our experiments).

Integrating Eq. (2), the evolution of each crystalline form can be obtained as

$$\xi_i(t) = k_i(t) - \int_0^t \left(\xi(s)\frac{dk_i(s)}{ds}\right)ds \qquad (i = \alpha \text{ or } meso) \quad (4)$$

Of course, if only one crystalline phase is considered (1 phase model), Eq. (3) describes the evolution of its volume fraction with time.

Kolmogoroff equation was adopted in this work to describe the evolution of the volume fraction crystallized toward α form [5]

$$k_\alpha(t) = \frac{4\pi}{3}\int_0^t \frac{dN(s)}{ds}\left[\int_s^t G(u)du\right]^3 ds \qquad (5)$$

where N and G represent nucleation density and spherulitic growth rate, whose dependence upon time is described by the functions $N(s)$ and $G(u)$ in Eq. (5).

Kolmogoroff equation can not be adopted for the mesomorphic form as the structure of this form has not been clarified yet [6]. The Avrami–Evans–Nakamura kinetic equation is the most commonly adopted in the literature to describe the crystallization kinetics toward the mesomorphic form [9], since a minimum set of parameters is needed to describe the kinetics by this approach; thus, the evolution of the undisturbed volume of mesomorphic phase was described as

$$k_{meso}(t) = \ln 2\left[\int_0^t A(T(s))ds\right]^n \qquad (6)$$

where n is the Avrami index and $A(T)$ a kinetic constant, which, on the basis of isokinetic assumption, is simply described by a Gaussian shaped curve (D, T_{max} and K_0 are half width of the Gaussian curve, temperature at which the maximum of $A(t)$ is attained and the maximum value itself, respectively)

$$A(T) = K_0 \exp\left[-4\ln 2\frac{(T - T_{max})^2}{D^2}\right] \qquad (7)$$

Secondary crystallization is not accounted for in the current model formulation. It is assumed, thus, that in the whole set of data collected in this work secondary crystallization does not have a significant effect on crystallinity degree. It should be pointed out, however, that all data were collected within a few hours after solidification.

4. Tuning of kinetic parameters

4.1. Crystallization kinetics from optical measurements

Nucleation density and growth rate measurements were performed on the resin adopted in this work, at University of Genoa by optical microscopy. Samples were sandwiched between 2 microscope slides in a hot stage at 503 K and annealed for 15 min; they were then cooled down (at a rate of about 1 K/s) until the desired isothermal crystallization temperature was reached (temperature of 394, 396, 398, 400, 403, 405 and 407 K were adopted). Nucleation density was determined by counting the nuclei in the sample and growth rate was determined by measuring the diameter of spherulites as a function of time until impingement took place. Experimental determinations showed that, as often found for commercial polymers, nucleation resulted to be predetermined, that is a fixed number of nuclei appeared at
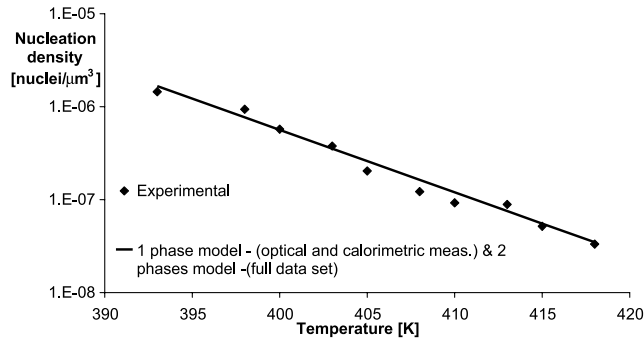
Fig. 11. Comparison between experimental determinations (by optical measurements) of nucleation density (symbols) and predictions performed by the model (lines), adopting parameters listed in Tables 1 (1 phase model) and 2 (2 phase model).

the test temperature, and their number did not change in time. Furthermore, spherulite radius growth rate was found constant with time at each test temperature. Growth rate and nucleation density vs temperature are reported in Figs. 11 and 12, respectively (symbols represent experimental data). In the range of temperatures investigated, both growth rate and nucleation density decrease on increasing temperature of the isothermal test [25].

Consistently with experimental determinations, and following literature indications [22,25], time dependence of growth rate and nucleation density in Eq. (5) may be expressed through temperature changes by adopting the following equations

$$G[T(t)] = G_0 \exp\left[-\frac{U}{R(T(t) - T_\infty)}\right]$$

$$\exp\left[-\frac{K_g(T(t) + T_m)}{2T(t)^2(T_m - T(t))}\right] \qquad (8)$$

$$N(T(t)) = N_0 \exp[\beta(T_m - T(t))] \qquad (9)$$

It is not the purpose of this paper to discuss the equations adopted for growth rate and nucleation density theoretically. Eq. (9) in particular, empirically describes an exponential variation of the number of heterogeneous nuclei with the temperature [22], as often reported for iPP.

Eq. (9) accounts also of athermal nucleation, since growth starts in this type of nucleation as soon as fixed size of embryos become critical during cooling; according to Eq. (9) nucleation rate during a cooling procedure can be expressed as

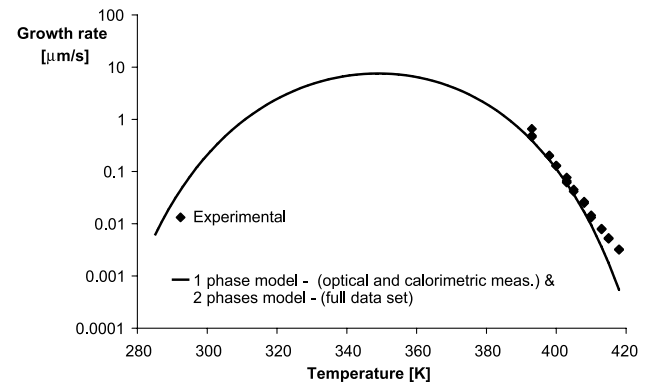$$N = \frac{dN}{dt} = -\beta N(T)T \qquad (10)$$

Fig. 12. Comparison between experimental determinations (by optical measurements) of spherulitic growth rate (symbols) and predictions performed by the model (lines), adopting parameters listed in Tables 1 (1 phase model) and 2 (2 phase model).

4.2. First tuning of kinetic parameters

A first attempt to improve the kinetic model was performed by identifying the parameters on the basis of optical microscopy and calorimetric data, simultaneously. In the range of cooling rate attainable by DSC apparatus only α phase forms; thus, only the kinetic equation of the α form was taken into account (1 phase model). Since T_m was identified as 467 K and $\chi_{m,\alpha}$ was found to be 55%, the only parameters needed to describe crystallization kinetics of the α form by means of the model presented above are G_0, K_g, U/R, T_∞, N_0 and β.

The values of the parameters found by best fitting on optical and DSC data are reported in Table 1. The fit of data was obtained by minimization of the difference between the model calculation and the experimental points reported in Figs. 1, 2, 11 and 12, each data point being equally weighted in the fit. A unique set of parameters is obtained if one fits all data simultaneously. It is worth noticing that the values found for N_0, β, U/R and T_∞ are consistent with literature indications [13,22]. Model predictions and experimental data (symbols) are compared in Figs. 1, 2, 5, 7, 11 and 12. As expected, model results give a good description of all isothermal data, of DSC cooling ramps and of experimental data taken on samples obtained at low cooling rates; vice versa, for cooling rates higher than about 20 K/s comparison becomes quite poor (as shown in Figs. 5 and 7) since maximum value of crystallinity degree is always reached by model predictions even at the highest applied cooling rates, when the data show that both density and percentage of α phase undergo a relevant decrease.

Indeed, considering α phase only (1 phase model), it was not possible to identify a reliable set of parameters able to

Table 1
List of parameters adopted in the model to describe experimental data according to '1 phase model'

N_0	β	K_g	G_0	T_{inf}	$\chi_{m,\alpha}$	U/R
17.4×10^6 nuclei/m^3	0.155 K^{-1}	534858 K^2	2.1×10^{10} μm/s	236 K	0.55	755 K

satisfactorily describe optical observations, DSC data and the drop of both, density and percentage of α phase shown by experimental results at cooling rates higher than 20 K/s.

4.3. Complete optimization of kinetic parameters

A full 2 phases model accounting of the evolution of α and mesomorphic phases was than considered on the basis of whole set of data including phase distribution in quenched samples as reported in Fig. 7. Parameters for the description of α phase were left unchanged with respect to those identified in the previous step and a best fitting procedure was performed to identify the parameters of the mesomorphic phase (n, K_0, T_{max}, and D in Eqs. (6) and (7)) by minimization of the quadratic error between the whole set of data and of the two phases model predictions. The values of parameters identified are listed in Table 2 and are consistent with data reported in the literature as far as mesomorphic form is concerned.

Model predictions obtained by adopting the 2 phase model are reported in Figs. 1, 2, 5, 7, 11 and 12. The whole set of data is now satisfactorily described. This means that a correct description of the evolution of the α phase during solidification can be attained by means of the presented model only if the evolution of the competing mesomorphic phase is kept into account.

Evolutions of α and mesomorphic volume fractions as predicted by the model during tests carried out at cooling rates of 50 and 90 K/s (see Figs. 4 and 9) are reported in Fig. 13. During the cooling test carried out at 50 K/s, as shown in Fig. 13, crystallization starts at 350 K toward the α form and goes on until about 310 K when the kinetic of the mesomorphic form becomes faster. For the cooling rate of 90 K/s the resin starts to crystallize at about 340 K toward α phase, but at about 330 K α phase is overcome by a faster kinetic toward the mesomorphic form.

The comments to the curves of Fig. 13 should be compared with half times of the evolution of two phases during isothermal tests. In an ideal isothermal test, if only kinetics of mesomorphic phase were active, according to Eqs. (3) and (6), being the kinetic constant function of temperature only, the half time (i.e. the time at which the volume fraction has reached one half of maximum value) would be the reciprocal of the kinetic constant $A(T)$. If, vice versa, only crystallization toward α form were active, as nucleation density and growth rate are functions of temperature only, according to Eqs. (3) and (5), crystal-

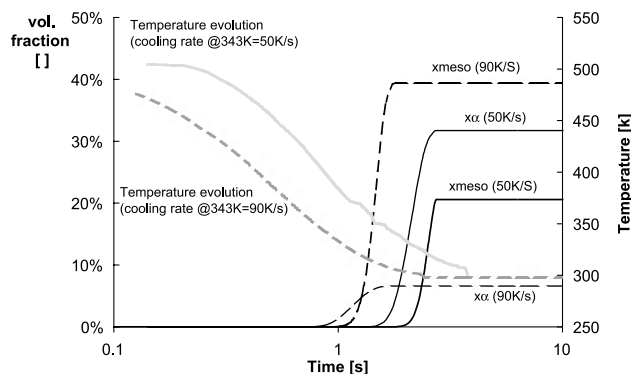Fig. 13. Evolutions of α and mesomorphic volume fraction as predicted by the model during tests carried out at cooling rates of 50 and 90 K/s.

lization half time $t_{0.5}$ can be written as

$$t_{0.5}(T) = \frac{1}{G(T)} \sqrt[3]{\frac{3 \ln 2}{4 \pi N(T)}} \qquad (11)$$

Half-times for both phases (α and mesomorphic) vs temperature are reported in Fig. 14. At higher temperatures, kinetics of α phase is faster than that of mesomorphic phase. At temperatures smaller than 333 K which are reached during fast cooling tests, crystallization kinetics of the mesomorphic phase becomes faster than that of the α phase. These features are consistent with the evolution of crystallinity during the two quenches at 50 and 90 K/s considered in Fig. 13. It is worth noticing that, at least for temperatures higher than 373 K, where reliable data of α phase crystallization half times are available in Refs. [5,18], results for α phase reported in Fig. 14 compare well with kinetic data usually found for iPP.

The kinetic model and its parameters reported in Table 2 were identified on the basis of a very wide and diversified set of data, including results of the analysis of samples solidified under cooling rates of a few hundreds K/s. The evolution of crystallinities during solidification of these samples would be a very valuable piece of information, unfortunately, at the moment, cooling ramps at these cooling rates are not available to experimental observation.
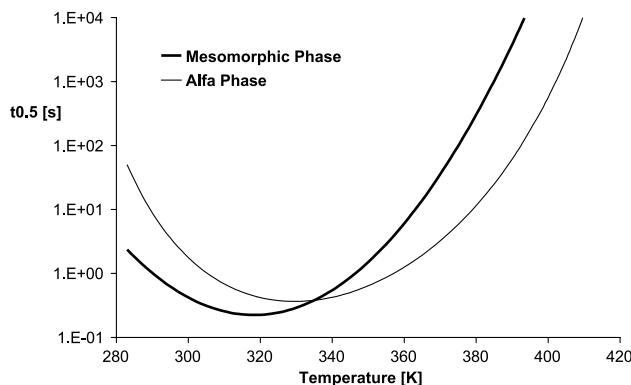

Fig. 14. Half times for the evolution of the two phases during two ideal isothermal tests in which only one crystalline phase is kept into account.

Table 2
List of parameters adopted in the model to describe experimental data according to '2 phase model'

$\chi_{m,meso}$	n	T_{max}	K_0	D
0.44	2.83	318 K	4.4 s^{-1}	38.3 K

If main features of the resin kinetic crystallization behavior are properly described by the model, at room temperature volume fractions of each of the two phases would reach maximum value within very short times, of the order of those reported in Fig. 14. Thus, also at the highest cooling rates to room temperature the α crystallization phase can be prevented from crystallizing to $\chi_{m,\alpha}$ only by effect of a faster kinetic process toward the mesomorphic phase, competing for the available amorphous.

5. Description of solidified structure

Fractional crystallinity of α phase, ξ_α can be interpreted also as the volume occupied by spherulites, per unit volume. The ratio between fractional crystallinity and the number of active nuclei per unit volume is therefore an average measure of the final volume of spherulites. Correspondently average final radius of spherulites made of α crystallites can be calculated as

$$\bar{R} = \sqrt[3]{\frac{3\xi_{\alpha,final}}{4\pi N_{a,final}}} \qquad (12)$$

where $N_{a,final}$ is the final number of active nuclei, which can be calculated from $N(T)$ as [5]

$$N_{a,final} = \int_0^{t_{final}} \frac{dN[T(s)]}{ds}(1 - \xi(s))ds \qquad (13)$$

Eq. (13) simply states that final number of spherulites can be obtained by summing up all nuclei formed during previous history in the volume fraction available to amorphous phase.

Measured diameters of spherulites are compared in Fig. 10 with model predictions obtained by adopting each of the two sets of parameters identified above. As clear from Fig. 10, if the optimization of kinetic parameters is performed considering optical microscopy and DSC data, a satisfactory agreement is attained in the whole range of cooling rates considered. It should be considered, however, that according to this model (identified as 1 phase model) a fully spherulitic volume is predicted, even at the highest applied cooling rates, where SEM images show that no impingement occurred. If parameters of the kinetic model are tuned on the basis of all available data (2 phase model), model results satisfactorily describe experimental data for almost all solidification conditions, including spherulites diameters.

6. Conclusions

A kinetic model was developed in this work on the basis of a very wide and diversified set of experimental data: DSC carried out under both isothermal and non-isothermal conditions; optical determinations of nucleation density and spherulites growth rate; density measurements and analysis of X-ray spectra of samples solidified at controlled cooling rates (up to 300 K/s at 343 K).

The model accounts for the formation of two competing phases: alpha and mesomorphic. Kolmogoroff equation was adopted to describe the crystallization rate of the α form, identifying appropriate equations for nucleation density and spherulite growth rate. Avrami–Evans–Nakamura kinetic equation was, vice-versa, adopted to describe the evolution of the mesomorphic phase. Resulting kinetic model satisfactorily describes the whole set of experimental data, including those obtained on samples solidified under cooling rates as high as those encountered by polymers during processing operations.

Model results show that a correct description of the evolution of the α phase during solidification at cooling rates higher than a few K/s can be attained only if the evolution of the competing mesomorphic phase is kept into account. Furthermore, at room temperature, volume fraction of each of the two phases would reach its maximum value within very short times, of the order of few seconds. Thus, also during very fast cooling procedures to room temperature, crystallization of the α phase is prevented from attaining the maximum possible value only by effect of a faster kinetic process toward the mesomorphic phase, which competes for the available amorphous volume.

Diameters of spherulites in samples solidified under different cooling rates were obtained by analyzing of SEM micrographs. Experimental dependence of spherulite diameters upon cooling rate satisfactorily compares with predictions based on the kinetic model identified.

References

[1] Ozawa T. Kinetics of non isothermal crystallization. Polymer 1971; 12(3):150–8.

[2] Ziabicki A. Crystallization of polymers in variable external conditions. Part 1. Colloid Polym Sci 1996;274(3):209–17.

[3] Nakamura K, Watanabe T, Katayama K, Amano T. Non isothermal crystallization of polymers. I. Relation between crystallization temperature, crystallinity, and cooling conditions. J Appl Polym Sci 1972;1077–91.

[4] Malkin AYA, Beghishev VP, Keapin IA, Bolgov SA. General treatment of polymer crystallization kinetics—Part 1. A new macrokinetic equation and its experimental verification. Polym Engr Sci 1984;24(18):1394–401.

[5] Eder G, Janeschitz-Kriegl H. In: Meijer HEM, editor. Materials science and technology, vol. 18. New York: Wiley; 1997.

[6] Vittoria V. Properties of iPP. Handbook of polymer science and technology; 1989.

[7] Brucato V, Piccarolo S, Titomanlio G. Crystallization kinetics in relation to polymer processing. Makromol Chem, Macromol Symp 1993;245–55.

[8] Piccarolo S, Brucato V, Kifliem Z. Non-isothermal crystallization kinetics of PET. Polym Engr Sci 2000;40(6):1263–72.

[9] Piccarolo S, Alessi S, Brucato V, Titomanlio G. Crystallization behaviour at high cooling rates of two polypropylenes in crystallization of polymers. Dordrecht: Kluwer Academic Publishers; 1993. p. 475–80.

[10] Piccarolo S, Saiu M, Brucato V, Titomanlio G. Crystallization of

polymer melts under fast cooling. II High-purity iPP. J Appl Polym Sci 1992;46:625–34.

[11] Pantani R, Titomanlio G. Description of PVT behaviour of an industrial polypropylene–EPR copolymer in process conditions. J Appl Polym Sci 2001;80:267–78.

[12] Coccorullo I, Gorrasi G, Pantani R. Structural organization and transport properties of iPP/LLDPE blends solidified at controlled cooling rates. J Appl Polym Sci 2001;2237–44.

[13] Isayev AI, Catignani BF. Crystallization and microstructure in quenched slabs of various molecular weight polypropylenes. Polym Engr Sci 1997;37(9):1526–39.

[14] Ding Z, Spruiell JE. J Polym Sci, Part B 1996;34:2783.

[15] Madkour TM, Mark JE. Modeling of the crystallization of isotactic polypropylene chains. J Polym Sci: Part B: Polym Phys 1997;35: 2757–64.

[16] Brucato V, De Santis F, Lamberti G, Titomanlio G. A new method for on-line monitoring of non isothermal crystallization kinetics of polymers. Polym Bull (Berl, Germany) 2002;48(2):207–12.

[17] Xu J, Srinivas S, Marand H, Agarwal P. Equilibrium melting temperature and undercooling dependence of the spherulitic growth rate of isotactic polypropylene. Macromolecules 1998;31:8230–40.

[18] Hieber CA. Correlation for the quiescent crystallization kinetics of isotactic polypropylene and polyethyleneterephthalate. Polymer 1995; 36(7):1455–67.

[19] Dorset DL, McCourt MP, Kopp S, Schumacher M, Okihara T, Lotz B. Isotactic polypropylene, β-phase: a study in frustration. Polymer 1998;39(25):6331–7.

[20] Meille SV, Phillips PJ, Mezghani K, Bruckner S. $\alpha-\gamma$ Disorder in isotactic polypropylene crystallized under high pressure. Macromolecules 1996;(29):795–7.

[21] Choi C, White J. Correlation and modeling of the occurrence of different crystalline forms of isotactic polypropylene as a function of cooling rate and uniaxial stress in thin and thick parts. Polym Engr Sci 2000;40(3):645–55.

[22] Angello C, Fulchiron R, Douilard A, Chabert B, Fillit R, Vautrin A, David L. Crystallization of isotactic polypropylene under high pressure (γ phase). Macromolecules 2000;33:4138–45.

[23] Murthy NS, Minor H. General procedure for evaluating amorphous scattering and crystallinity from X-ray diffraction scans of semicrystalline polymers. Polymer 1990;31(6):996–1002.

[24] White HM, Basset DC. On row structures, secondary nucleation and continuity in alpha polypropylene. Polymer 1998;39(14):3211–9.

[25] Coccorullo I, Petrosino P, Pantani R, Alfonso GC, Titomanlio G. Crystallisation kinetics and structure formation in polymers under high cooling rates. Proceedings of INSTM Meeting, Trento; June 2001.